JOURNAL

OF THE AMERICAN CHEMICAL SOCIETY

VOLUME 104, NUMBER 19 SEPTEMBER 22, 1982

NMR Studies of Self-Association of Disodium Guanosine 5′-Monophosphate

Steffen B. Petersen,[†,§] Jens J. Led,*[†] Eric R. Johnston,[‡,∥] and David M. Grant[‡]

Contribution from the Department of Chemical Physics, University of Copenhagen, The H. C. Ørsted Institute, DK-2100 Copenhagen Ø, Denmark, and the Department of Chemistry, University of Utah, Salt Lake City, Utah 84112. *Received January 13, 1982*

Abstract: The self-association of the disodium salt of guanosine 5′-monophosphate has been studied by ^{1}H, ^{13}C, and ^{31}P NMR spectroscopy. The chemical shift, ^{1}H spin–lattice relaxation, and saturation-transfer measurements and Mn^{2+}-induced line broadenings are inconsistent with previously proposed models in which self-associated GMP consists of stacks of planar hydrogen-bonded tetramers or continuously hydrogen-bonded helices. Instead, the results are consistent with a model wherein stacking of monomers is the predominant mode of interaction at higher temperatures, whereas at lower temperatures stacks of asymmetric hydrogen-bonded dimers form. With further lowering of temperature, a second incompletely characterized complex, possibly a stacked, symmetric dimer, forms. The ^{13}C spectrum of 5′-GMP,Na_2 in the gel state strongly indicates that the hydrogen-bonded asymmetric dimer is also the fundamental unit in the gel phase.

Guanosine 5′-monophosphate (5′-GMP) differs in many respects from other nucleotides.[1-5] In particular, gel formation is unique for guanosine and its derivatives.[1,2] The X-ray fiber-diffraction patterns of the disodium salt of 5′-GMP have been interpreted in terms of a continuously hydrogen-bonded helix with 15 nucleotides in four turns,[5] whereas the 3′-GMP isomer in the gel state is found to form stacks of planar hydrogen-bonded tetramers.[3] 5′-GMP precipitated from a 1.3 M NaCl solution gave an X-ray fiber-diffraction pattern similar to the pattern obtained for poly(guanosine),[6] which has also been interpreted in terms of stacking of planar hydrogen-bonded tetramers. In none of these X-ray studies, however, has interaction with the cation been included in the model. The ^{1}H NMR spectra of the salts 5′-GMP,X_2 (X = Na, K, Rb) are significantly different for different X at low temperature and high 5′-GMP concentration as shown by Pinnavaia et al.,[7] who also studied the concentration and temperature dependence of the 220-MHz ^{1}H NMR spectra of 5′-GMP,Na_2.[8] Likewise, two new signals were observed in the ^{31}P NMR spectrum of 5′-GMP,Na_2 at low temperature.[9] Further, it has been found that the potassium salt forms the most stable self-associate.[7,10] Laszlo et al.[9,10] report a dramatic increase in the ^{23}Na resonance line width upon formation of the 5′-GMP,Na_2 self-associate, indicating that Na^+ binds to the complex. Also a K^+-induced broadening of the ^{23}Na NMR signal in 0.1 M 5′-GMP,Na_2 was reported.[10] On the basis of these results a planar hydrogen-bonded tetrameric model was proposed,[7-10] and all the observed resonance positions of the H8 protons were interpreted in terms of stacking of tetramers and electrostatic effects of the doubly charged phosphate groups.

In the present study, NMR data are presented that clearly contradict the tetrameric model and the continuously hydrogen-bonded helix model. In contrast, the data are consistent with a model wherein stacking of monomers is the predominant mode of interaction at higher temperatures, whereas stacks of hydrogen-bonded asymmetric dimers form as the temperature is lowered. In addition, the data show that a second complex, possibly a stacked, symmetric dimer, forms at even lower temperatures.

Experimental Section

Preparation of Solutions. The disodium salt of 5′-GMP (Sigma), twice lyophilized from 99.5% D_2O, was used without further purification for the ^{1}H and ^{31}P NMR measurements. Solutions were prepared by dissolving the appropriate amount of the salt in 99.5% D_2O. EDTA (1

[†] University of Copenhagen.
[‡] University of Utah.
[§] Present address: Department of Chemistry, State University of New York at Stony Brook, Stony Brook, NY 11794.
[∥] Present address: Department of Chemistry, University of Washington, Seattle, WA 98195.

(1) Chantot, J. F.; Guschelbauer, W. *Jerusalem Symp. Quantum Chem. Biochem.* **1972**, *4*, 205–214.
(2) Guschelbauer, W. *Jerusalem Symp. Quantum Chem. Biochem.* **1972**, *4*, 297–309.
(3) Gellert, M.; Lipsett, M. N.; Davies, D. R. *Proc. Natl. Acad. Sci. U.S.A.* **1962**, *48*, 2013–2018.
(4) Brahms, J.; Aubertin, A. M.; Dirheimer, G.; Gruberg-Manago, M. *Biochemistry* **1969**, *8*, 3269–3278.
(5) Sasisekharan, V.; Zimmerman, S.; Davies, D. R. *J. Mol. Biol.* **1975**, *92*, 171–179.
(6) Zimmerman, S. B. *J. Mol. Biol.* **1976**, *106*, 663–672.
(7) Pinnavaia, T. J.; Marshall, C. L.; Mettler, C. M.; Fisk, C. L.; Miles, H. T.; Becker, E. D. *J. Am. Chem. Soc.* **1978**, *100*, 3625–3627.
(8) Pinnavaia, T. J.; Miles, H. T.; Becker, E. D. *J. Am. Chem. Soc.* **1975**, *97*, 7198.
(9) Borzo, M.; Detellier, C.; Laszlo, P.; Paris, A. *J. Am. Chem. Soc.* **1980**, *102*, 1124–1134.
(10) Detellier, C.; Laszlo, P. *J. Am. Chem. Soc.* **1980**, *102*, 1135–1141.

0002-7863/82/1504-5007$01.25/0

mg/mL of solution) was added to bind possible paramagnetic impurities. For the ^{13}C measurements the appropriate amount of 5′-GMP,Na_2 was dissolved in H_2O and 1 mg of EDTA added per mL of solution. The Mn^{2+}-containing samples were prepared by dissolving the appropriate amount of salt in a $MnCl_2 \cdot 4H_2O$ (Merck p a) solution in D_2O.

NMR Measurements. Proton spectra were obtained with a Varian SC 300 spectrometer operating at 300 MHz. Solvent D_2O provided the internal deuterium lock. ^1H chemical shifts are reported relative to an external Me_4Si reference without correction for bulk susceptibility changes. After each experiment, the temperature was measured with a methanol sample that was allowed to equilibrate in the probe for 15 min. The delay time between pulses was 25 s, and the duration of the applied 90° pulses was 8 μs. A total of 16K data points were used to define the 3-kHz spectral window.

The 500-MHz spectra were obtained on a Bruker WH 500 instrument. The delay time between pulses was 30 s, and the duration of the applied 90° pulses was 8 μs. A total of 16K data points were used to define the 3-kHz spectral range. ^1H spin–lattice relaxation times were obtained at 300-MHz with an inversion–recovery pulse sequence, and T_1 values were obtained at 3 and 9 °C from the partially relaxed spectra by using a three-parameter regression analysis.

Proton-saturation transfer experiments were performed at 3 °C and 300 MHz on the Varian SC 300 spectrometer. To minimize spillover effects due to the finite bandwidth of the frequency synthesizer, we first set the irradiating frequency downfield of H8D by an amount equal to the chemical shift difference between H8D and H8C, and the power level at which H8D exhibited detectable intensity loss was determined. A slightly lower power level was then used in the saturation transfer experiments and was sufficient to ensure complete saturation. Intensities for saturation transfer and T_1 measurements were peak heights obtained from digitized spectra. Results of saturation transfer experiments are reported as fractional intensity losses $t_i(j) = [I^0_i - I_i(j)]/I^0_i$, where I^0_i is the equilibrium intensity of spin i and $I_i(j)$ is its steady-state intensity when site j is saturated.

Carbon-13 NMR spectra were obtained at 75.5 MHz on a Varian SC 300 spectrometer and at 67.89 MHz on a Bruker 270 spectrometer. At 75.5 MHz, the delay time between pulses was 5.2 s. The proton decoupling irradiation was applied only during the 0.96-s acquisition time to prevent sample heating. Duration of the applied 30° pulses was 8 μs. A total of 32K data points defined the 17-kHz spectral range. At 67.89 MHz, the applied 30° pulses were 7 μs and 64K data points defined the 17-kHz spectral range. Sample temperatures were measured by employing the diffeence in chemical shift between the ^{13}C signals of CCl_4 and the carbonyl carbon of acetone-d_6 in a 50/50 vol % mixture of the two compounds.[11] The mixture was contained in a sealed 5-mm NMR tube coaxially placed in the 10-mm sample tubes.

^{31}P spectra were obtained with a Varian XL 100 spectrometer operating at 40.5 MHz. The pulse delay time was 25 s, and the duration of the 90° pulses was 100 μs. A total of 4K data points defined the 500-Hz spectral window. The temperature was measured with a thermocouple immersed in the sample immediately after obtaining the spectrum. During this measurement the decoupler was turned off.

The effect of Mn^{2+} on the phosphorus spectra was investigated by using a JEOL FX 90Q spectrometer operating at 36.24 MHz. The pulse delay was 4.2 s, and the 90° pulse duration was 3 μs. A total of 16K data points defined the 2-kHz spectral range. The temperature was measured with a thermocouple as described above.

Results

^{13}C Spectra of the Purine Region. ^{13}C NMR chemical shifts were measured as a function of concentration (Figure 1) and temperature (Figure 2). As shown in Figure 1, all purine carbons shift upfield when the concentration of 5′-GMP is increased, indicating that stacking is the predominant mode of interaction in the observed concentration range.[12] Figure 2 also shows that upfield shifts are observed for all purine carbons in a 0.2 M 5′-GMP,Na_2 solution when the temperature is decreased. However, when the 5′-GMP concentration is raised to 0.5 M, the ^{13}C NMR spectrum shows several new peaks below 30 °C. Thus, as may be seen in Figure 3A,B a total of ten new peaks is observed in the purine region. In all cases the new lines disappear at temperatures above 30 °C. Since the purine ring contains five carbons, the data suggest that 5′-GMP is exchanging slowly among three magnetically inequivalent sites. Futhermore, when the temperature is lowered from 26 to 18 °C, a significant increase in the populations of the new sites is observed as judged from intensity ratios. Further lowering of the temperature (Figure 3C) leads to the merging of C6B and C6D as well as of C4B and C2D. At 9 °C (Figure 3D), a third new set of peaks appears (the five C peaks), demonstrating that a third new site becomes significant. These new peaks are well separated from the A, B, and D peaks except in the case of C2, where C2B and C2C coalesce. The

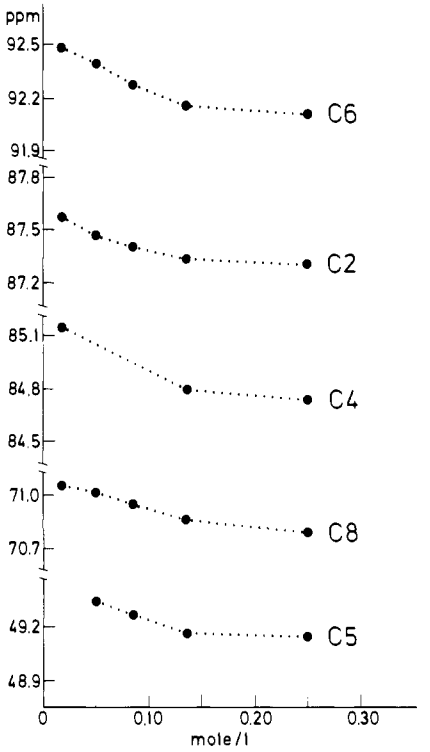

Figure 1. ^{13}C chemical shifts at 273 K and pH 7.0 of the purine carbons as a function of the 5′-GMP,Na_2 concentration. The measured shifts are relative to 1,4-dioxane as internal reference.

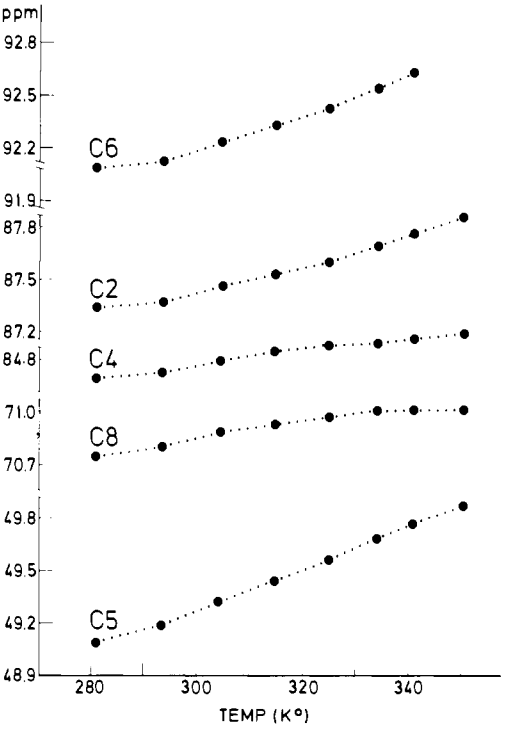

Figure 2. ^{13}C chemical shifts of the purine carbons in a 0.2 M 5′-GMP,Na_2 solution as a function of the temperature. The measured shifts are relative to 1,4-dioxane as internal reference.

(11) Led, J. J.; Petersen, S. B. *J. Magn. Reson.* **1978**, *32*, 1–17.
(12) Smith, I. C. P.; Mantsch, H. H.; Lapper, R. D.; Deslauriers, R.; Schleich, T. *Jerusalem Symp. Quantum Chem. Biochem.* **1973**, *5*, 381–401.

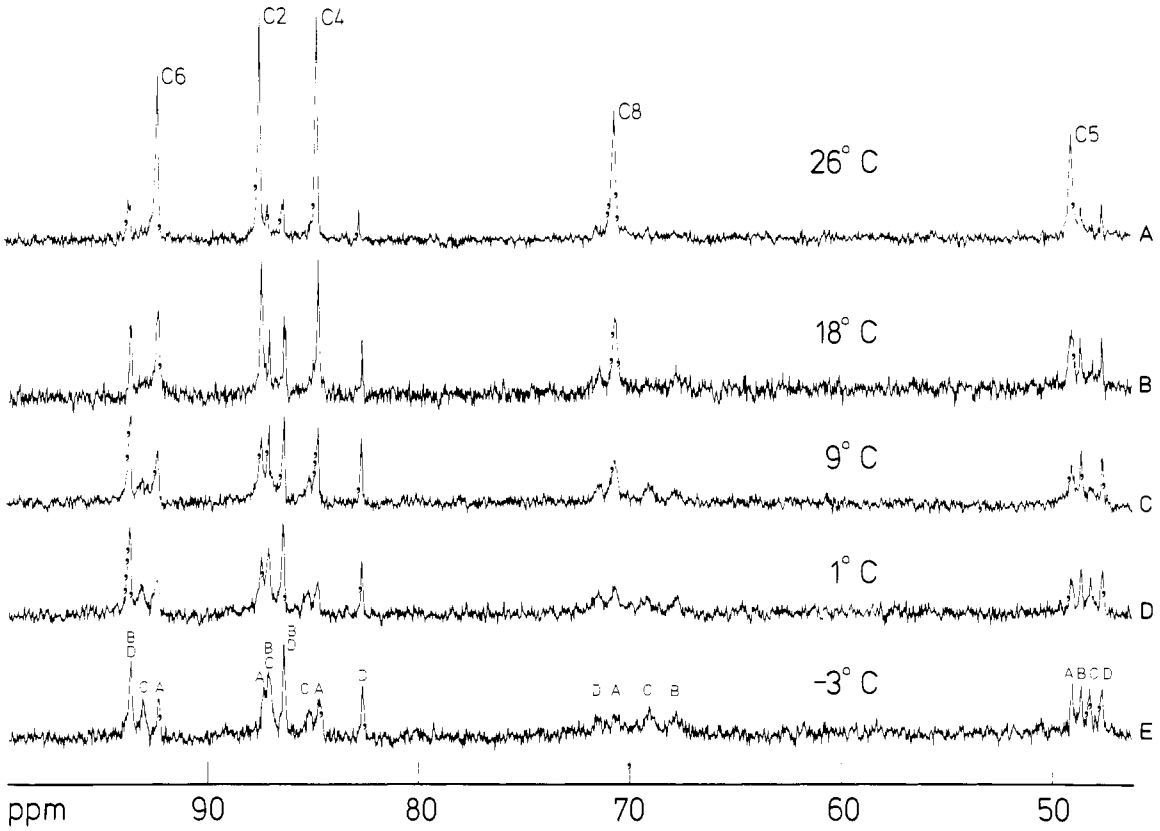

Figure 3. Purine region of the 75.5-MHz ^{13}C NMR spectra of a 0.5 M 5′-GMP,Na_2 solution as a function of temperature. The measured shifts are relative to 1.4-dioxane as internal reference.

appearance of these new lines is also reversible. Thus the ^{13}C data shows that four magnetically nonequivalent purine environments exist at temperatures below 10 °C.

^1H Spectra of the Purine Region. The 300- and 500-MHz ^1H NMR spectra of the purine region are essentially identical with spectra published by other workers.[7-9] The ^1H NMR spectra of the purine region demonstrate the existence of at least four magnetically nonequivalent sites at temperatures below 20 °C.

^{13}C Spectra of the Ribose Region. The ^{13}C spectra of the ribose region show several new peaks when the temperature is lowered. At least seven new signals are observed at 1 °C in 0.5 M 5′-GMP,Na_2, as shown in Figure 4. When the temperature is lowered, the parent peak C1′ appears to lose intensity relative to C4′, and simultaneously a total of at least three new lines is observable in the C1′–C4′ region. The C2′ parent peak splits into two peaks in the same temperature interval. Even at low temperature, the C3′ peak appears sharp. However, the area of the C3′ resonance decreases significantly as compared to the area of the C4′ resonance when the temperature is lowered. This intensity reduction is accompanied by the appearance of two new peaks in the vicinity of the C3′ parent peak. A similar pronounced decrease in intensity with decreasing temperature is observed for the C5′ parent peak. Concurrent with this change, a broad peak appears downfield relative to the C5′ parent peak.

^1H Spectra of the Ribose Region. The ^1H NMR spectrum at 300 MHz of the ribose region is shown as a function of temperature in Figure 5. As may be seen in this figure, no J couplings are observable at 24 °C. Also, a sharp downfield and a broad upfield resonance are observed in the vicinity of the H1′ parent signal. At 8 °C the central peak in the H1′ region splits into two signals, and at 4 °C the H1′ region separates into four distinct lines. The H2′ parent signal loses intensity when the temperature is lowered, and simultaneously the peak that at 24 °C appears as a downfield shoulder on the H2′ parent signal develops into the major signal in the H2′ region. The H3′ resonance remains a relatively sharp signal throughout the same temperature interval except at the lowest temperatures, where a splitting into two signals of similar intensity is observed. The same observation is made

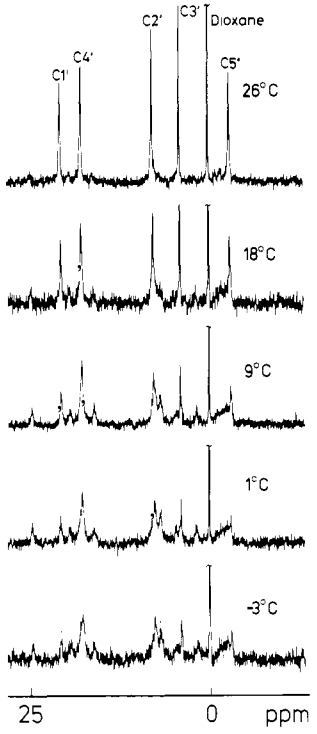

Figure 4. Ribose region of the 75.5-MHz ^{13}C NMR spectra of a 0.5 M 5′-GMP,Na_2 solution as a function of temperature. The measured shifts are relative to 1,4-dioxane as internal reference.

for the H4′ region. Thus at 4 °C, the H4′ signal is split into two resonances of equal intensity. A further temperature decrease to −1 °C leads to a concerted increase in the intensity of the downfield component and a decrease of the upfield component. The H5′ peak differs markedly from the rest of the ribose region. In the entire temperature range from 24 to −1 °C, it remains a

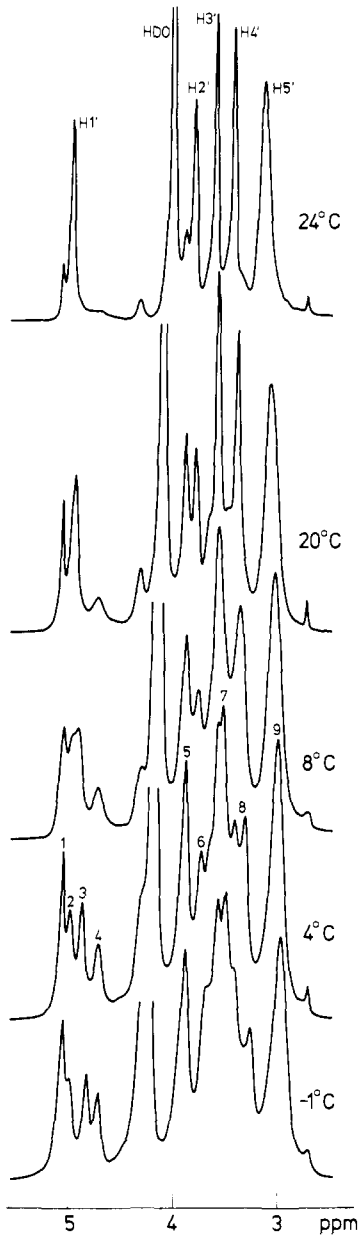

Figure 5. Ribose region of the 300-MHz ^1H NMR spectra of a 0.5 M 5′-GMP,Na_2 solution as a function of temperature. The measured shifts are relative to Me_4Si as external reference.

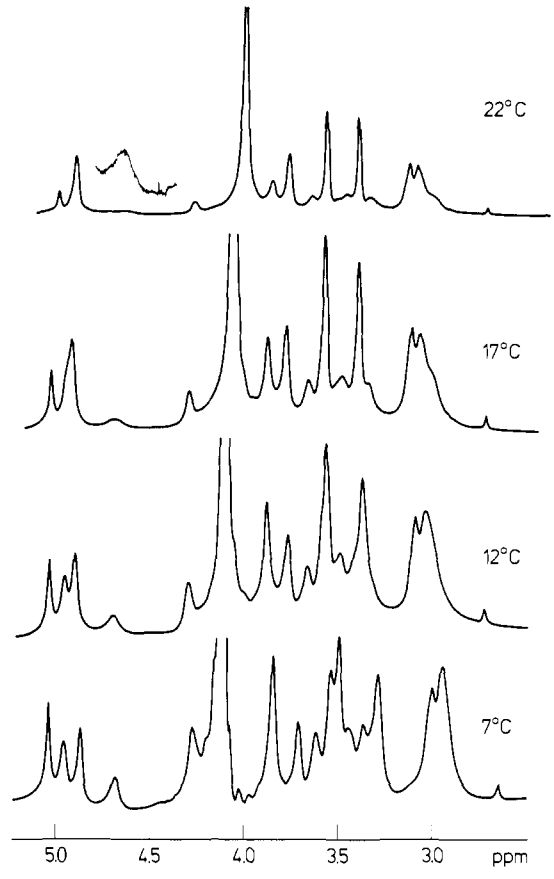

Figure 6. Ribose region of the 500-MHz ^1H NMR spectra of a 0.5 M 5′-GMP,Na_2 solution as a function of temperature. The measured shifts are relative to Me_4Si as external reference.

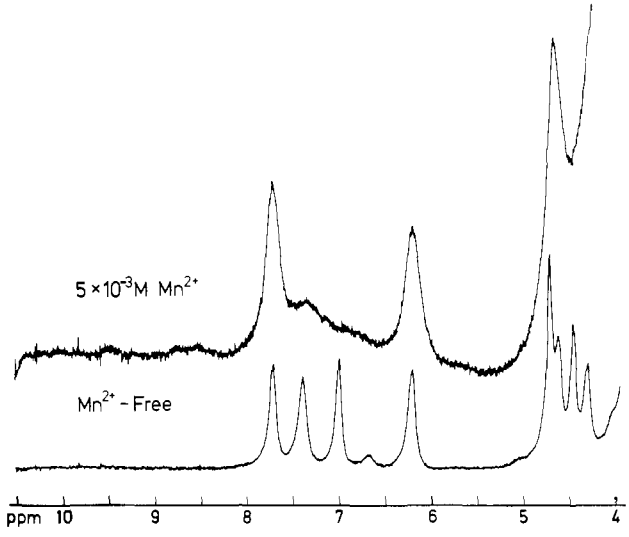

Figure 7. Purine region of the 300-MHz ^1H NMR spectra at 3 °C of a 0.5 M 5′-GMP,Na_2 solution 5×10^{-3} M in Mn^{2+} (top) and a 0.5 M solution of 5′-GMP,Na_2 without Mn^{2+} added (bottom). The measured shifts are relative to Me_4Si as external reference.

single peak although it broadens considerably. However, at 500 MHz (Figure 6) the H5′ resonance is split into three signals that coalesce into two signals at low temperature. Also, as compared to the 300-MHz spectra, two additional lines are observed in the H3′ region. Thus a total of 16 proton resonances is observed in the ribose region at 500 MHz and 7 °C, indicating that at least three magnetically different ribose environments exist at this temperature.

^{31}P NMR Spectrum. The 36.2-MHz NMR spectrum of a 0.5 M 5′-GMP,Na_2 solution at 9 °C is shown in the upper trace of Figure 9. Two new signals of equal area appear, and their areas increase at the expense of the parent signal when the temperature is further lowered. This result indicates that the ribose phosphate group exists in at least three magnetically different environments, as previously concluded by Laszlo et al.[9]

Interaction of Mn^{2+} with 5′-GMP. As can be seen in the ^1H spectra of 5′-GMP,Na_2 shown in Figure 7, the addition of Mn^{2+} has a pronounced effect on the two central peaks in the H8 region, whereas the outer two H8 lines are only slightly broadened. In agreement with this Pinnavaia et al.[8] have reported that addition of 10^{-3} M Mn^{2+} or Cu^{2+} preferentially shortens the relaxation time of the third highest field line relative to the two outer signals. Also, as shown in Figure 8, all parent (A) purine ^{13}C signals as well as the parent signal of C5′ are broadened beyond detection in the presence of 5×10^{-3} M Mn^{2+}. In Figure 9 it is seen that addition of 1×10^{-4} M Mn^{2+} broadens the parent peak in the ^{31}P spectrum considerably, whereas the two new peaks of equal area appear only slightly broadened.

T_1 Results. In Table I are listed the spin–lattice relaxation rates measured at 300 MHz for a number of ^1H lines at 3 and 9 °C in a 0.5 M solution of 5′-GMP,Na_2. At both temperatures, the

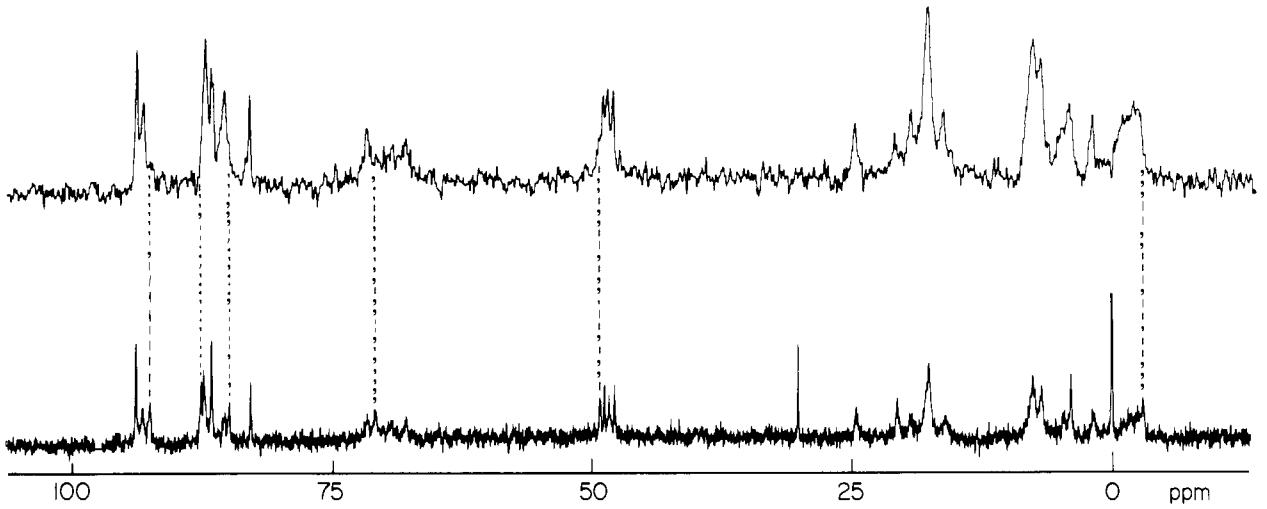

Figure 8. 75.5-MHz ^{13}C NMR spectra at 3 °C of a 0.5 M 5'-GMP,Na_2 solution 5×10^{-3} M in Mn^{2+} (top) and 0.5 M 5'-GMP,Na_2 solution without Mn^{2+} added (bottom). The dashed lines indicate the positions of parent peaks.

Table I. Relaxation Rates for Selected Proton Lines

	$1/T_1$[a]	
	3 °C	9 °C
H8D	0.271	0.281
	±0.029	±0.084
H8C	0.619	0.676
	±0.038	±0.019
H8A	0.574	0.657
	±0.033	±0.029
H8B	0.288	0.318
	±0.026	±0.007
1[b]	0.306	0.288
	±0.032	±0.001
2[b]	0.297	0.311
	±0.030	±0.016
3[b]	0.513	0.493
	±0.030	±0.025
4[b]	0.477	0.557
	±0.033	±0.014

[a] In s^{-1} at 300 MHz for a 0.5 M solution of 5'GMP,Na_2. [b] Proton resonances in the H1' region (see Figure 5). The given rates are uncorrected for possible effects of peak overlaps.

T_1 values for the H8 signals and those in the H1' region are clearly divided into two sets. For the H1' signals, only apparent T_1 values, uncorrected for peak overlap, are given. The T_1 values for the two central H8 lines are almost identical and only half the value of the T_1's for the two outer lines, which are likewise similar. Pinnavaia et al.[8] have also measured T_1 values for the H8 proton signals at 19 °C, 220 MHz, and 0.59 M 5'-GMP. Despite significant overlap of the two centeral H8 lines under these conditions, they also concluded that the T_1's of the H8 signals are divided into two sets.

Saturation Transfer Results. Selective irradiation of one of the H8 lines produces a reduction in all other signal intensities, as shown by the data collected in Table II. In particular, selective irradiation of the H8 signals also demonstrates that the H8 lines can be divided into two sets: saturation of an outer signal primarily affects the other outer signal, whereas saturation of an inner line primarily affects the other inner line. Moreover, these transfers

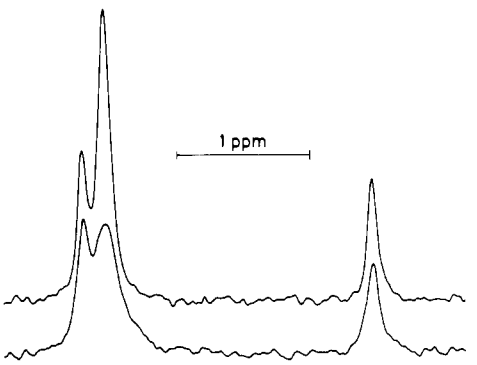

Figure 9. 36.24-MHz ^{31}P NMR spectra at 9 °C of a 0.5 M 5'-GMP,Na_2 solution 10^{-4} M in Mn^{2+} (bottom) and a 0.5 M 5'-GMP,Na_2 solution without Mn^{2+} added (top).

of saturation are symmetric. In addition, irradiation of an H8 line results in a significant reduction of signal intensities in the ribose region.

^{13}C Spectrum of Gelified 5'-GMP,Na_2. In Figure 10 is shown the 75.5-MHz ^{13}C spectrum of a gelified 0.5 M 5'-GMP solution at 3 °C and pH 7. As may be seen in this figure, several of the peaks in the gel spectrum coincide in chemical shift with the new peaks observed in the nongelified solution, indicating a similar origin of the new peaks in the two cases.

Discussion

The observation of upfield shifts for the ^{13}C signals with decreasing temperature at constant concentration (Figure 2) indicates that stacking is a predominant mode of interaction.[12] This interpretation is further supported by the observation of ^{13}C upfield shifts for all purine carbons when the concentration of 5'-GMP is increased at constant temperature (Figure 1). The ten new peaks observed in the ^{13}C spectrum of the purine region at 26 °C (Figure 3) indicate that, in addition to simple stacking, new molecular species are being formed. Since the observed changes are reversible, various types of self-association schemes are candidates in the search for the origin of these new signals. Stacking is known

Table II. Observed Saturation Transfers at 3 °C for 0.5 M 5'-GMP,Na_2 at 300 MHz[a]

	obsd reduction												
irradiated	H8D	H8C	H8A	H8B	1	2	3	4	5	6	7	8	9
H8D		0.17	0.19	0.40	0.35	0.37	0.20	0.22	0.36	0.15	0.17	0.17	0.11
H8C	0.29		0.64	0.28	0.23	0.22	0.28	0.33	0.31	0.34	0.23	0.19	0.17
H8A	0.28	0.69		0.26	0.17	0.16	0.30	0.28	0.29	0.36	0.25	0.24	0.21
H8B	0.49	0.26	0.19		0.51	0.51	0.26	0.31	0.41	0.09	0.21	0.23	0.15

[a] Peak assignments are as given in Figures 5 and 7 (lower spectrum).

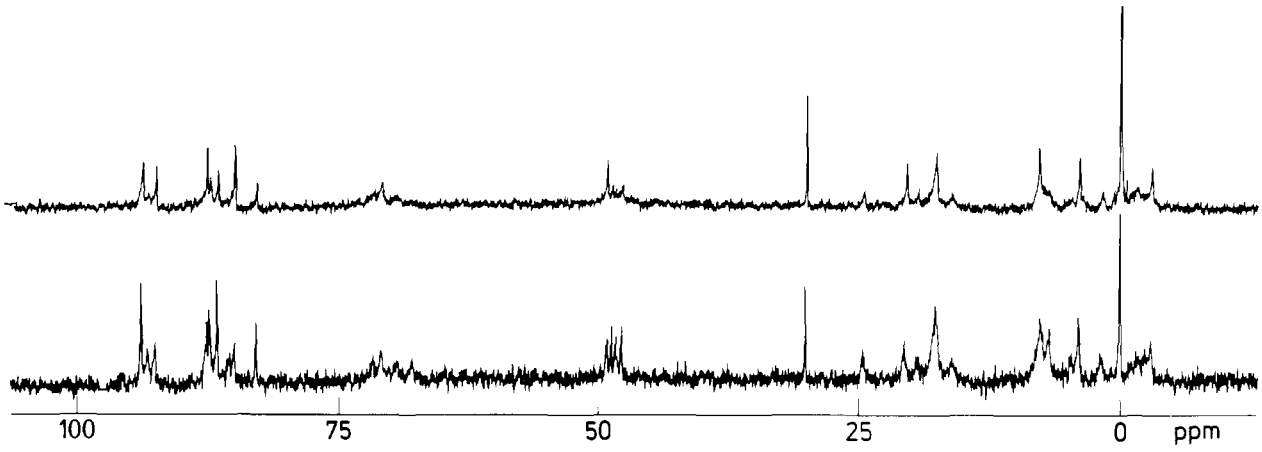

Figure 10. 75.5-MHz ^{13}C NMR spectra at 3 °C of 0.5 M 5′-GMP,Na_2 at pH 8 (bottom) and gelified 0.5 M 5′-GMP,Na_2 at pH 7 (top).

to give rise to upfield shift contributions of less than 2 ppm.[12,13] Hydrogen bonding induces down- or upfield shifts on the order of 2 ppm or less in the purine ring when guanosine forms a Watson–Crick base pair with cytidine.[14] Therefore, assuming that stacking and purine–purine hydrogen bonding are the only modes of self-association, new lines will appear less than 4 ppm from their parent peaks. Thus in the case of C5, C6, and C8, the assignment of new peaks is straightforward. Further, the new peak appearing upfield of C4 is assigned to a new C4 resonance, since its separation from the C2 parent peak is more than 4 ppm. The three new lines appearing between C2 and C4 can only be assigned to either C2 or C4.

The significantly broader lines observed for the C8 lines compared to the other purine ^{13}C resonances (Figure 3) can be attributed to the fact that C8 is the only proton-bearing purine carbon. Thus the dipolar line broadening caused by an increasing correlation time with decreasing temperature will be greatest for C8, whereas the line widths of the quaternary purine carbons will be relatively less affected by ^1H–^{13}C dipolar line broadening and thus mostly dominated by magnetic field inhomogeneity.

Assuming that the conditions of slow chemical exchange are fulfilled, the formation of asymmetric dimers explains the appearance of two new signals of equal intensity in the vicinity of each of the parent peaks. Since hydrogen bonding is known[14] to produce downfield shifts of all guanosine carbons except C5, the observation of upfield shifts of the new signals of C4, C5, and C8 cannot be accounted for solely by hydrogen bonding. However, a combination of hydrogen bonding and stacking could explain the observation.

The Tetramer Models.[7-10] The models for 5′-GMP self-association involving stacking of planar hydrogen-bonded tetramers of 5′-GMP assign the B, C, and D signals in the H8 NMR spectrum (Figure 11) to tetramers in different types of ordered stacks, while the A signal is assigned to tetramers in rapid exchange with unassociated monomers or nonregular stacked aggregates. The observed shift of the A signal with decreasing temperature or increasing concentration is explained by this exchange process. The ordered stacking of tetramers increases with lower temperature and higher concentration. There are, however, several lines of evidence that make these tetramer models unlikely.

The tetramer models proposed by Pinnavaia et al.[7,8] involve head-to-tail stacking of three tetramer units (i.e., a dodecamer) or, alternatively, head-to-tail and head-to-head stacking of two tetramer units (i.e., two octamers). The dodecamer model, which assigns the B and D signals to the two outer tetramer units and the C signal to the central tetramer unit, does not agree with the saturation transfer data of the present study. Thus the data in Table II demonstrate that the C site exchanges predominantly with the A site and only to a much smaller extent (if at all) with the B and D sites. This observation is incompatible with C being

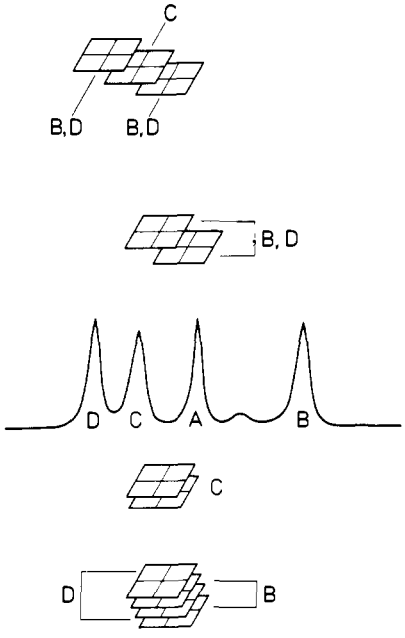

Figure 11. The assignment of the ^1H signals of H8 according to the tetramer model.[7-10]

the central unit in a dodecamer, since there appears to be no facile mechanism that would allow the central tetramer unit to exchange directly with the A-parent tetramer. The octamer model, which presumably assigns two of the self-structure signals to tetramers in head-to-tail position and the third signal to tetramers in a head-to-head arrangement, also seems unlikely. Thus for this model, one would only expect exchange between the self-structure signals (B, C, and D) and the A signal and not between two self-structure signals, as is found experimentally (B and D).

In another version of the tetramer model proposed by Laszlo et al.,[9,10] the B and D signals were assigned to the two "inner" and the two "outer" tetramers, respectively, of a hexadecamer, while the C signal was attributed to a symmetric (head to head) dimer. Also, this model is in conflict with the data of Table II, as again there appears to be no plausible mechanism that would allow direct interchange between the B and D sites without involving the intermediacy of either A or C.

As for the chemical shifts of the self-structure lines, downfield shifts relative to the parent peak have been observed for a number of B and D signals in both the ^1H and the ^{13}C spectra. This observation, however, is inconsistent with a model that exclusively involves stacking of tetramers, since this mode of association is expected to produce only upfield shifts. Although electrical field effects stemming from the charged phosphate group could introduce downfield shifts on nuclei in its immediate vicinity,[15] it

(13) Giessner-Prettre, C.; Pullman, B. *J. Theor. Biol.* **1970**, *27*, 87–95.
(14) Petersen, S. B.; Led, J. J. *J. Am. Chem. Soc.* **1981**, *103*, 5308–5313.

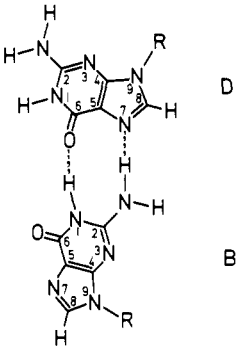

Figure 12. Asymmetric hydrogen-bonded dimer of 5'-GMP.

does not seem possible to construct a model of stacks of tetramers in which the phosphate group is close to all the nuclei for which downfield shifts are observed, that is C2, C4, C8, and H8.

It is clear from Figure 7 that Mn^{2+} interacts strongly with the parent A site and the C site and only to a considerably smaller degree with the B and D environments. In addition, the data presented here demonstrate that the ribose phosphate group of the C complex is very similar to the parent phosphate group in chemical shift and ability to bind Mn^{2+}, implying that the ribose phosphate conformation in these two species is the same. These observations are inconsistent with C being the central unit in a dodecamer as there is no plausible reason why Mn^{2+} should gain access to the central tetramer in a stack more easily than to the terminal tetramers. It also seems unlikely that no conformational restrictions should be imposed on the ribose groups of the internal unit in a dodecamer as compared to those of free tetramers. These observations are also inconsistent with B and D being the inner and the outer units of a symmetric hexadecamer, as one might expect the outer units to bind Mn^{2+} more readily than the inner units; yet B and D bind manganese to the same (small) extent.

Finally, the C signal of C6 is observed downfield relative to the C6A parent signal, indicating that binding in the C complex involves hydrogen-bond formation close to C6. This observation is also at variance with the tetramer models, which in general predict upfield shifts of new lines relative to parent lines.

We therefore conclude that the tetramer models are unable to explain (1) the observed downfield shifts of most new lines relative to the parent signals in the ^{13}C spectrum; (2) the substantial chemical exchange between C and A and between B and D, but not between C and B–D or between A and B–D; (3) the selectivity of the manganese-induced line broadenings; and (4) the chemical shift similarity between the ribose phosphate groups of the C complex and the A parent molecules.

The Helix Model.[5] The formation of a continuously hydrogen-bonded helix is presumed to follow the scheme[16]

$$(5'\text{-GMP})_n + 5'\text{-GMP} \rightleftharpoons (5'\text{-GMP})_{n+1}$$

where n is a positive integer. The first step in this process is the formation of an asymmetric hydrogen-bonded dimer (Figure 12), the second step a trimer, and the third step a chain tetramer. Further polymerization leads to formation of the helix. Considering the order of appearance as a function of temperature, we must assign the A signal to free monomer and the B and D signals to the two units of the asymmetric dimer or to the terminal units of the trimer, tetramer, and polymer, whereas the C signal must be attributed to the interjacent units of these associates. Thus, the larger the value of n, the more intense should be the C signal relative to the B and D signals. However, a C signal intensity only slightly larger than that of the B and D signals is observed at the lowest accessible temperature (−1 °C).[9] Likewise, the assignment of C to the relatively immobile interjacent units of a polymer disagrees with the saturation transfer results, since according to these data there is substantial exchange of the interjacent units with monomer. Also, it is difficult to explain why the ribose phosphate groups of the internal units of the helix (^{31}P NMR C signal) but not those of the terminal units (^{31}P B and D signals) have a chemical shift similar to that of free monomer (^{31}P A signal). A similar argument can be given for the observed selectivity in the Mn^{2+}-induced line broadenings. Hence we conclude that the helix model, like the tetramer models, is incompatible with the results obtained in the present study. Consequently, we propose an alternative model.

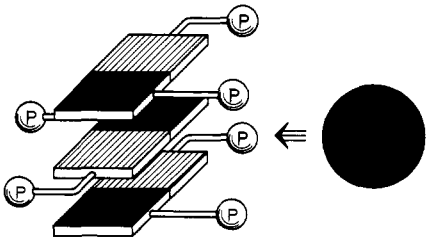

Figure 13. Sterical sketch of the stacked asymmetric hydrogen-bonded dimers of 5'-GMP. Each layer represents an asymmetric dimer. P denotes a phosphate group, and the large spherical body to the right represents a sodium ion.

Table III. 75.5-MHz ^{13}C Peak Positions, $\Delta\nu_S$, Measured Relative to the Parent Line[a]

carbon	$\Delta\nu_S$, Hz	ν_o, ppm	$\Delta\nu_H$,[b] Hz
2	−31, −31, −65	88.2	34
4	126, 27, −162	85.5	56
5	−31, −64, −106	49.5	−46
6	55, 100, 100	92.9	152
8	50, −125, −212	71.3	(0)

[a] Position of parent line given by ν_o. [b] $\Delta\nu_H$ is the hydrogen-bond shift as reported for the Watson–Crick base pair of guanosine and cytidine.[14]

Alternative Model for Self-Association of 5'-GMP. As mentioned earlier, only a combination of stacking and hydrogen bonding can explain the chemical shifts of the new signals. This concert of interaction is consistent with the observation that hydrogen bonding and stacking are cooperative phenomena in oligonucleotides.[17] Accordingly, we propose a model for the self-association of 5'-GMP that involves both hydrogen bonding and stacking and agrees in general with all the experimental data obtained in the present study as well as in previous studies.[7-10]

According to this model, monomers of 5'-GMP are in fast exchange with stacks of 5'-GMP above 30 °C, giving rise to the A signal. The size of these stacks is temperature dependent. Below 30 °C, interstack hydrogen bonding produces stacks of hydrogen-bonded asymmetric dimers, giving rise to the B and D signals. With further lowering of temperature, a second, as yet incompletely characterized, complex forms, producing the C signal.

One would expect that the phosphate groups in each layer of the stack are oriented in a direction opposite to that of the phosphate groups in the layers above and below, owing to charge repulsion. As sketched in Figure 13, this arrangement of asymmetric dimers creates a cation trap with four proximal negatively charged phosphate groups and possible additional binding sites (O6, N7) in the layer intersecting the two sets of phosphate groups.

We now consider the positions of the new lines relative to their parent lines (Table III). The new C5 lines all appear upfield relative to the parent C5A line, in agreement with the observation[14] that hydrogen-bonding and stacking shifts are both upfield for this carbon. The most upfield peak, C5D, is assigned to the 5'-GMP molecule hydrogen bonded at O6 and N7 (see Figure 12). In the case of C2, it seems unlikely that the hydrogen-bonding shifts of the two C2 carbons in the asymmetric dimer should be nearly equal, since one 5'-GMP unit is directly involved in hydrogen bonding at C2 whereas the other is not (Figure 12). Therefore, the two nearly coincident lines appearing at ca. 86.9

(15) Schweizer, M. P.; Broom, A. D.; Ts'O, P.O.P.; Hollis, D. P. *J. Am. Chem. Soc.* **1968**, *90*, 1042–1055.
(16) Klump, H. *Ber. Bunsenges. Phys. Chem.* **1976**, *80*, 121–124.
(17) Krugh, T. R.; Laing, J. W.; Young, M. A. *Biochemistry* **1976**, *15*, 1224–1228.

ppm are assigned to C2D and C4B. Likewise, the new C2 line at 87.1 ppm is assigned to the 5′-GMP unit hydrogen bonded at C2 and N1 (C2B). For C4 the assignment of the new peaks is tentative, since C4 is equally close to both hydrogen-bonding regions in the asymmetric dimer. The near coincidence of the two new C6 lines is interpreted as resulting from very similar hydrogen-bonding contributions to the C6 chemical shifts in the dimer, in which hydrogen bonding occurs at N1 in one unit and at O6 in the other unit.

The ribose group is also influenced by dimerization, as judged from the appearance of new lines in the ribose region of the ^{13}C, ^{1}H, and ^{31}P NMR spectra. The ^{31}P spectrum indicates that the phosphate groups of the dimer possess quite different magnetic environments. ^{31}P chemical shifts are known to be very sensitive to conformational changes,[18] and it is reasonable to expect different phosphate–ribose conformations for the two ends of the dimer.

Finally, the asymmetric dimer model explains the dramatic increase in the ^{23}Na NMR line width that occurs upon formation of the self-associate[9] in that the mobility of the sodium ion decreases when bound by the proximal phosphate groups (Figure 13), owing to the larger molecular weight of the stacked self-associate.

The appearance of a third new line below 9 °C in the vicinity of each parent line indicates that a second complex becomes significant in this temperature range. The absence of a third new line in the ^{31}P spectrum, even at the lowest temperatures, suggests that the ribose phosphate conformations for this second complex and the bulk monomer are similar. This is further supported by the ^{1}H and ^{13}C NMR spectra of the ribose region, both of which show significantly smaller multiplicity of lines at low temperature than do the corresponding spectra of the purine region. Thus only 12 lines representing five ribose protons are observed in the ^{1}H NMR spectrum, whereas 17 lines representing five purine carbons are observed in the ^{13}C spectrum. This result indicates that only three ribose environments exist, compared to four purine environments.

The interaction between Mn^{2+} and 5′-GMP involves, as one would expect, the phosphate group. However, as seen from Figure 9, the addition of 1×10^{-4} M Mn^{2+} leads to a significant broadening only of the parent line in the ^{31}P spectrum, whereas the effect on the lines presumably arising from the asymmetric dimer is considerably smaller. The ^{31}P C line (which is evidently coincident in chemical shift with the parent A line) is most probably broadened by Mn^{2+} to the same extent as the A line, since the joint ^{31}P signal, although broadened, is still Lorentzian. Likewise, the ^{1}H spectrum in Figure 7 demonstrates that the H8 A and C lines are selectively broadened by 5×10^{-3} M Mn^{2+}. These results are evidence that Mn^{2+} directly interacts with the phosphate groups in the bulk monomer and the C complex and that these groups are not strongly involved in sodium binding. Conversely, the phosphate groups in the B–D complex appear unable to bind Mn^{2+}.

The almost complete absence of the parent A lines in the purine region of the ^{13}C spectrum of the same solution indicates that Mn^{2+} is also binding at O6 and N7. This result is consistent with binding behavior observed for other nucleotides.[19] The ^{13}C purine C peaks, however, are essentially unbroadened by manganese. Thus N7 and O6 in the C complex are incapable of binding Mn^{2+}, possibly because they are engaged in hydrogen bonding of an as yet undetermined nature. Nevertheless, H8C is broadened, most likely as a result of dipolar interaction with Mn^{2+} bound at the C phosphate group. This in turn suggests that the conformation about the glycosidic bond in the monomer and the C complex is partially or predominantly anti. No conclusion concerning the glycosidic conformation in the B–D complex is possible.

The T_1 values of the H8B and H8D lines at 3 and 9 °C (Table I) are essentially equal and longer by a factor of 2 than the T_1's of the A and C species, which are also equal. The equality of T_1 for H8B and H8D is consistent with the asymmetric dimer model if the H8–ribose H dipolar interactions are comparable for H8B and H8D and the interactions are modulated by the (same) correlation time for approximately isotropic tumbling. The equality of T_1 for H8A and H8C is consistent with the H8–ribose H dipolar interactions being modulated primarily by rapid rotation about the N9–C1′ glycosidic bond at a rate that exceeds or is comparable to the rate of overall molecular tumbling and that is the same for the bulk monomer and the C complex. Moreover, since we are outside of motional narrowing (as judged from the inequality of T_1 and T_2 of the H8 lines), T_1 for H8B and H8D in this picture should be slightly longer than T_1 for H8A and H8C, as observed. Thus the T_1 data are consistent with a model in which the dimer ribose groups are locked in particular conformations, whereas the ribose groups of the bulk monomer and the C complex show essentially unconstrained mobility. The possibility that H8A and H8C have intrinsically different T_1 values that are averaged by chemical exchange can be excluded by the fact that transfer of saturation between H8A and H8C is symmetric (vide infra). Saturation transfer owing to chemical exchange between H8A and H8C would be asymmetric if T_{1A} and T_{1C} were markedly different.

The observed transfer of saturation among the H8 and ribose H signals at 3 °C is presented in Table II. Irradiation of H8A affects primarily H8C (and vice versa), whereas irradiation of H8B primarily affects H8D (and vice versa). Moreover, these transfers of saturation are symmetric. Transfer of saturation to the remaining H8 lines upon irradiation of one H8 line can be interpreted in terms of chemical exchange among the H8 sites (which are equally populated at 3 °C). Intensity decreases in the ribose region are intramolecular nuclear Overhauser enhancements (negative here since we are outside of motional narrowing)[20] resulting from H8–ribose H dipolar interaction. In view of the difficulties inherent in separating these contributions, no attempt to quantitatively interpret the saturation transfer data will be made here. However, neglect of intramolecular and intrastack NOE's and application of a simple model appropriate to two-site exchange[21] allow us to calculate approximate intersite rate constants $k_{AC} = k_{CA} = 1.2 \pm 0.2\ s^{-1}$, $k_{BD} = k_{DB} = 0.3 \pm 0.05\ s^{-1}$, $k_{AB} = k_{AD} = k_{DA} = k_{BA} \simeq 0.1 \pm 0.05\ s^{-1}$, and $k_{CB} = k_{CD} = k_{DC} = k_{BC} \simeq 0.1 \pm 0.05\ s^{-1}$. The error associated with exchange involving B–D and A and B–D and C is quite large, and the present data do not allow us to conclude that there is *direct* exchange between B–D and A or B–D and C. It is possible, for example, that the observed transfer of saturation of B and D upon irradiation of C is due entirely to exchange involving the intermediacy of A and not to direct exchange between B–D and C. Alternatively, exchange of A with B–D could require the intermediacy of C. Nevertheless, it is clear that significant direct exchange occurs between B and D and between A and C. The B–D exchange can be interpreted in terms of an opening and closing of the hydrogen bonds in the dimer units in such a way that the two units of the asymmetric dimer are interconverted. Concerted clockwise and counterclockwise rotation of the dimer units would produce such interconversion (Figure 12). The A–C exchange indicates that the C complex forms from bulk monomer at a rate at least tenfold greater than the rate at which the B–D complex forms from bulk monomer.

The general intensity decrease of approximately 50% that is observed in the ribose region upon irradiation of an H8 line is due to an intramolecular negative NOE that owing to chemical exchange and spin diffusion, is distributed throughout the ribose region. Assuming isotropic tumbling and only considering a simple two-spin dipolar interaction,[20] a negative NOE of ~ -0.5 at 300 MHz corresponds to a rotational correlation time $\tau_R \sim 1$ ns for the B–D and C complexes. Consideration of the inequality of T_1 and T_2[22] for the H8 lines at 3 °C (T_1/T_2 = 300, 160, 90, and 300

(18) Gorenstein, D. G. *J. Am. Chem. Soc.* **1975**, *97*, 898–900.
(19) Reddy, P. R.; Hamill, W. D.; Chheda, G. B.; Schweizer, M. P. *Biochemistry* **1981**, *20*, 4979–4986.
(20) Noggle, J. H.; Schirmer, R. E. "The Nuclear Overhauser Effect"; Academic Press: New York, 1971; Chapter 2.
(21) Forsén, S.; Hoffman, R. A. *J. Chem. Phys.* **1963**, *39*, 2892–2901.
(22) Farrar, T.; Becker, E. "Pulse and Fourier Transform NMR"; Academic Press: New York, 1971; Chapter 4.

for the H8 B, C, A, and D lines, respectively) yields approximate correlation times τ_R of 10 ns for the B–D complex, 7 ns for the C complex, and 5 ns for the bulk monomer. It is possible, as discussed above, that the correlation times for A and C refer primarily to ribose rotation and not to overall molecular tumbling. Firm evidence on this point is still forthcoming. For a 0.45 M solution of 5′-GMP at 0 °C, Borzo et al.[9] estimate a rotational correlation time averaged over all complexes of ~30 ns, on the basis of the observed line broadening of the ^{23}Na signal resulting from self-assembly.

The model proposed in the present study can account for the fact that a variety of cations is capable of inducing self-assembly. The cation trap schematized in Figure 13 is flexible due to the fact that the steric position of the constituent phosphate groups can be modified to accommodate a slightly smaller or larger cation. However, not all cations or complexation geometries seem feasible. Thus Mn^{2+} (r_I = 0.80 Å), although only slightly smaller than Na^+ (r_I = 0.96 Å), shows a greater affinity for the phosphate groups of the C complex and bulk monomer than for those of the asymmetric dimer, as dicussed above. This is indirect evidence that the cation binding site in the asymmetric dimer preferentially binds Na^+ to the exclusion of Mn^{2+}. Likewise, neither Li^+ (r_I = 0.60 Å) nor Cs^+ (r_I = 1.60 Å) is effective at inducing 5′-GMP self-assembly, whereas K^+ (r_I = 1.3 Å) is most effective.[7]

Nature of the C Complex. The structure of the C complex is presently unclear. Any proposed structure, however, must account for the following observations. First, the relative population of the H8C line, while smaller than that of either H8B or H8D at temperatures above ca. 9 °C, actually exceeds that of H8B or H8D at lower temperatures. Thus Laszlo et al. observed[9] relative populations of 27%, 31%, 15%, and 27% for H8B, -C, -A, and -D, respectively, in a 0.7 M solution of 5′-GMP at 0 °C. We have observed similar relative populations in a 0.5 M solution of 5′-GMP at 1 °C. This observation discounts the possibility that a third monomer is binding to each asymmetric dimer at low temperature, since limiting signals of equal population for H8B, H8C, and H8D would then be expected, and this is not observed. We can likewise discount the possibility that H8C is associated with a second signal (call it E) of equal area (in the same manner that B and D are associated) and coincident in chemical shift at all temperatures with the A monomer resonance, since the limiting low-temperature spectrum would contain equal C and A(E) lines, and this also is not observed.

Second, the H8C line exhibits a substantial downfield shift with decreasing temperature,[7,9] unlike H8B or H8D, whose chemical shifts are temperature independent. In the ^{13}C NMR spectrum (Figure 3), the C line of C8 appears upfield of the parent line, indicating that hydrogen-bond activity at N7 is negligible, whereas the C lines of C4 and C6 appear downfield of their respective parent lines, indicating that hydrogen bonds involving the six-membered ring are being formed. The Mn^{2+}-binding and T_1 data presented above demonstrate that the ribose phosphate group of the C complex is conformationally similar to that of bulk monomer and capable of binding Mn^{2+}, whereas Mn^{2+} does not bind at the purine ring of the C complex. This contrasts with the behavior observed for bulk monomer, which binds Mn^{2+} at O6 and N7. Finally, the saturation transfer results demonstrate substantial direct exchange between C and bulk monomer but do not permit an unequivocal determination of the existence of direct exchange between C and B–D. One intriguing possibility suggested by these observations is that C is a stacked, symmetric dimer formed by hydrogen bonds between N1H and O6. At the present time, however, firm evidence in support of this structure is lacking.

The Gel Structure. It is apparent from a comparison of the ^{13}C spectra in Figure 10 that both the asymmetric dimer and the parent monomer coexist in the gel phase. Thus the asymmetric dimer also appears to be the fundamental unit the gel structure.

Conclusion

Previously proposed models for the self-association of 5′-GMP,Na_2 involving either limited stacks of planar hydrogen-bonded tetramers or a continuous hydrogen-bonded helix are incompatible with the results of the present study. We conclude instead that stacking of monomers is the predominant mode of interaction above 30 °C, whereas below this temperature, stacks of asymmetric hydrogen-bonded dimers form. At even lower temperatures, an additional complex, possibly a stacked, symmetric dimer, forms. The latter complex exchanges directly with bulk monomer, whereas the units of the asymmetric dimer exchange only slowly with bulk monomer and more rapidly with each other. Mn^{2+} interacts with the phosphate groups of only the C complex and bulk monomer; the phosphate groups of the B–D complex strongly bind Na^+ to the exclusion of Mn^{2+}. The results do not permit a determination of the exact stacking geometry in the asymmetric dimer nor do they permit a determination of the exact nature of cation binding in this complex. An X-ray study of the gel structure of 5′-GMP in which the location of Na^+ ions in the complex is considered would be most valuable. NMR studies of the H-bonded, exchangeable protons in these complexes are planned to obtain further structural and dynamic information.

Acknowledgment. We thank the Danish Natural Science Research Council for support of the Bruker HX 270 and JEOL FX 90Q spectrometers used in the present study as well as the Bruker WH 90 spectrometer used in preliminary experiments. The 500-MHz ^1H NMR spectra were obtained on a Bruker WH 500 instrument at the California Institute of Technology, Pasadena, CA, with the kind hospitality of Professor Sunny I. Chan. Helpful discussions with Professor Martin P. Schweizer and Dr. Charles Mayne are gratefully acknowledged. S.B.P. was the recipient of a travel grant from the Danish Natural Scienc Research Council. The National Institutes of General Medical Sciences (PHS), under Grant GM 08521-20, also provided support for this work. Finally, we thank the referees for some critical comments.

Registry No. Disodium guanosine 5′-monophosphate, 5550-12-9.